Princeton Plasma Physics Laboratory

PPPL-4060

PPPL-4060

Prompt Loss of Energetic Ions during Early Neutral Beam Injection in the National Spherical Torus Experiment

S.S. Medley, D.S. Darrow, D. Liu,
and A.L. Roquemore

March 2005

Prepared for the U.S. Department of Energy under Contract DE-AC02-76CH03073.

PPPL Report Disclaimers

Full Legal Disclaimer

Trademark Disclaimer

PPPL Report Availability

This report is posted on the U.S. Department of Energy's Princeton Plasma Physics Laboratory Publications and Reports web site in Fiscal Year 2005. The home page for PPPL Reports and Publications is: http://www.pppl.gov/pub_report/

Office of Scientific and Technical Information (OSTI):

Available electronically at: http://www.osti.gov/bridge.

Available for a processing fee to U.S. Department of Energy and its contractors, in paper from:

U.S. Department of Energy
Office of Scientific and Technical Information
P.O. Box 62
Oak Ridge, TN 37831-0062

Telephone: (865) 576-8401

Fax: (865) 576-5728

E-mail: reports@adonis.osti.gov

National Technical Information Service (NTIS):

This report is available for sale to the general public from:

U.S. Department of Commerce
National Technical Information Service
5285 Port Royal Road
Springfield, VA 22161

Telephone: (800) 553-6847

Fax: (703) 605-6900

Email: orders@ntis.fedworld.gov

Online ordering: http://www.ntis.gov/ordering.htm

Prompt Loss of Energetic Ions during Early Neutral Beam Injection in the National Spherical Torus Experiment

S. S. Medley, D. S. Darrow, D. Liu*, and A. L. Roquemore

Princeton Plasma Physics Laboratory, Princeton, New Jersey, 08543, USA

* *University of California, Irvine, CA USA*

Email: ***medley@pppl.gov***

Abstract

Early neutral beam injection is used in the National Spherical Torus Experiment (NSTX) to heat the electrons and slow current penetration which keeps q(0) elevated to avoid deleterious MHD activity and at the same time reduces Ohmic flux consumption, all of which aids long pulse operation. However, the low plasma current ($I_p \sim 0.5$ MA) and electron density ($n_e \sim 1x10^{13}cm^{-3}$) attending early injection lead to elevated orbit and shine through losses. The inherent orbit losses are aggravated by large excursions in the outer gap width during current ramp up. An investigation of this behavior using various energetic particle diagnostics on NSTX and TRANSP analysis is presented.

1. Introduction

In the National Spherical Torus Experiment (NSTX) [1,2], advanced operational techniques are employed to induce H-mode during discharge initiation, including early neutral beam injection near the time of a brief pause or “flat-spot” in the current ramp up [3]. This scheme aids in the attainment of long pulse discharges by reducing flux

consumption and delaying the onset of deleterious MHD activity [4]. The reason for this behavior is straightforward. The electron temperature profile broadens thereby reducing the plasma resistance to slow Ohmic current penetration and preserve an elevated core safety factor (q), thus increasing MHD stability. The pressure profile broadens which increases the bootstrap current, saving flux consumption. The broader pressure profile also permits the achievement of higher β by delaying onset of deleterious MHD activity.

The magnetic field topology in contemporary spherical tokamaks can cause substantial prompt loss of energetic ions, particularly at low plasma current levels. Spherical tokamaks operate at significantly lower magnetic field than do most tokamaks; e.g. B_T = 0.3 - 0.6 T in NSTX compared to 2 – 5 T in conventional aspect ratio tokamaks. In conventional tokamaks, the poloidal magnetic field strength typically is much less than the toroidal field. As a result, the radial excursion of an energetic ion drift orbit is roughly the size of a poloidal gyroradius, which is considerably greater than the size of the Larmor radius. In spherical tokamaks, however, the poloidal magnetic field strength can exceed that of the toroidal field and the radial extent of the drift orbit can be comparable to the Larmor orbit. For example, the gyroradius of 80 keV D co-injected NB heating ions in NSTX can be ~ 0.3 m at the outboard midplane of the plasma. This is a sizable fraction of the 0.68 m minor radius for a typical plasma.

The prompt loss of neutral beam ions from NSTX [5] is expected to be between 12% and 42% of the total beam power, depending on the plasma current (1 MA to 0.6 MA). Such losses are diagnosed either from temperature measurements of ion deposition on first wall structures or by Faraday cup probes [6] which detect ions on loss orbits. Losses of ions with energy above 1 keV in NSTX have been measured with a Faraday cup

probe located at the vessel midplane [7]. In addition to this prompt loss to first-wall structures, orbit excursions beyond the separatrix combined with high atomic and molecular density enveloping the plasma can result in a depletion of the energetic ion population due to the energy-dependent charge-exchange losses.

2. Diagnostic Observations of NB Turn-0n Energetic Ion Loss

In this section, the diagnostics used on NSTX to directly measure the energy distribution of confined and lost ions are described first and then measurements indicative of ion loss during early neutral beam injection are presented.

The Neutral Particle Analyzer(NPA) diagnostic on NSTX [8] utilizes a PPPL-designed EIIB spectrometer [9] which measures the mass-resolved energy spectra of H and D neutrals simultaneously with a time resolution of ~1 ms set by signal-to-noise levels. The calibrated energy range is E = 0.5 – 150 keV and the energy resolution varies from $\Delta E/E$ = 7% at low E to $\Delta E/E$ = 3% at high E. The detector consists of a large area microchannel plate that is provided with two rectangular, semi-continuous active area rows for detecting H and D. Each mass row has 39 energy channels. The NPA measures Maxwellian spectra of residual hydrogen in deuterium plasmas to obtain ion temperatures [10] and deuterium energetic ion spectra produced by neutral beam (NB) injection into deuterium plasmas [11]. As shown in Fig. 1, the NPA views across the co-injection paths of the three neutral beam lines on NSTX that inject at R_{NB} of ~ 0.7 m (source A), ~ 0.6 m (source B) and ~ 0.5 m (source C). In NSTX, by convention the neutral beam tangency radii are positive for *injection* in the co-direction. On the other hand, the convention adopted for the

NPA is that positive sightline tangency radii correspond to *viewing* co-directed ions. The horizontal scanning capability for the NPA over a sightline tangency range of R_{tan} = 1.25 m to R_{tan} = - 0.75 m has enabled measurement of the anisotropic energy distribution of the beam ions.

A solid state Neutral Particle Analyzer (ssNPA) array [12] installed on the NSTX also measures the energy distribution of energetic NB particles. The array consists of four chords viewing through a common vacuum flange. The tangency radii of the viewing chords are 60, 90, 100, and 120 cm. They view across the three co-injection neutral beam lines on NSTX and detect co-going energetic ions. The present detectors are silicon photodiodes and the count rate is limited to $2x10^5$ cps due to saturation of the signal processing electronics. The calibrated energy range is 40 ~ 129 keV, the energy resolution is ~ 10 keV and the time resolution is ~ 1 ms.

The scintillator Fast Lost Ion Probe (sFLIP) [13] on NSTX is a magnetic spectrometer that employs a combination of ambient magnetic field and aperture geometry to disperse ions of different pitch angles and energies onto a sclntillator plate. The image on the plate is transferred through a 50 x 50 fiber optic bundle to a CCD camera. Through orbit analysis, the distribution of the energetic ion image on the scintillator is related to the gyroradius (or energy) and pitch angle of the lost ions. The energy resolution is ~ 80 keV, the pitch angle resolution is ~ 6^o and the time resolution is ~ 16 ms.

Fig. 2 illustrates the generic signature that is observed on the NPA signal due to energetic ion loss attending early NB injection. Shown is the NPA flux signal at E_D = 70 keV and the waveform for neutral beam injection. Source B with E_b = 88 keV us turned on at t = 50 ms followed by Source A with E_b = 88 keV at 200 ms. Initially the NPA signal

shows a “normal” rise but then suddenly drops by ~ 70% followed by a recovery phase up to turn-on of the second beam. This turn-on drop is not a detector saturation effect, since even higher signal levels are sustained after turn-on of the second NB. The second beam may also exhibit turn-on loss, but very modest compared with the first beam.

Discharges with early (SN112157 in red) and late (SN112088 in blue) NB injection are compared in Fig. 3. During the time of interest up to t ~ 300 ms, both discharges are similar with regard to plasma current, electron density, beam energy, injected power and outer gap evolution. For late injection, the NPA signal and the neutron rate rise smoothly to a plateau. For early injection, however, the initial rise in the NPA signal quickly collapses and neutron production is minimal.

Fig. 4 shows the 3D spectrum of the NPA flux versus deuterium ion energy and time for the late injection case. The point to note is that following beam turn-on the flux rises smoothly at all energy and rolls over to an equilibrium distribution. However, for the early injection case shown in Fig. 5, the 3D spectrum of the NPA flux versus deuterium ion energy and time rises promptly at all energies but then collapses and “wobbles” (encircled region). When the second beam is turned on at t = 200 ms, the flux rises smoothly and rolls over to an equilibrium distribution as seen in the late turn-on case in Fig. 4.

The NPA signal is shown for a selection of channels in the energy range $E_b/2 < E \leq E_b$) for SN112157 in Fig. 6. The solid red and blue lines mark the turn-on of the first and second beams, respectively. The dashed lines track the delay, Δt, in signal peaking with decreasing energy that is simply the effect of classical ion slowing down. The slowing-down time on electrons first defined by Spitzer [14] is given by

$$\tau_{se} = 6.27 \times 10^{14} \frac{A_b T_e^{3/2}}{Z_b^2 n_e \ln \Lambda_e}. \quad (1)$$

E_{crit} , the critical energy at which ions and electrons receive a equal energy transfer from the beam ions, is given by

$$E_{crit} = 14.8 A_b T_e \left(\frac{[Z_i]}{A_i} \right)^{2/3} \quad (2)$$

where the average charge to mass ratio of the bulk ions (denoted by the subscript '*i*') is

$$\frac{[Z_i]}{A_i} = \frac{\sum_j n_j (Z_j^2 / A_j) \ln \Lambda_j}{n_e \ln \Lambda_e} \quad (3)$$

and the subscript '*j*' indexes the bulk and impurity ion species. Units in the above expressions are time(s), energy(eV), mass(AMU), T_e(eV) and n_e(m^{-3}).

For SN112157 shown in Fig. 6, at t_1 = 0.08 s, Te ~ 200 eV and n_e ~ $1.2 \times 10^{19} m^{-3}$ while at t_2 = 0.17 s, Te ~ 600 eV and n_e ~ $2.1 \times 10^{19} m^{-3}$. From Eq. 1 and using $\ln\Lambda$ ~ 15, the calculated ratio of slowing-down times is τ_1 / τ_2 ~ 28 ms/58 ms ~ 0.48, which agrees reasonably well with the measured value of 0.5 (measured over only a portion of the energy slowing-down range). This provides supporting evidence that the NPA signal is "real" (e.g. not a detector saturation effect).

The evolution of the ssNPA and EIIB NPA signals around the time of early injection are compared in Fig. 7 for discharge SN113192. Source B injected at t = 70 ms and Source A at t = 170 ms, both with E_b = 99 keV and P_b = 2.4 MW. The center column in red shows the ssNPA signals for a range of deuterium energies and the right-hand column in blue gives the matching EIIB signals. As is evident, the solid state Neutral Particle Analyzer (ssNPA) on NSTX exhibits a similar time evolution following early beam injection as the EIIB NPA, except the signal drop appears to be somewhat deeper than that of the NPA. Since different detectors are used in the two systems, this provides further evidence against detector saturation effects.

ORBIT code analysis shows that prompt orbit loss occurs when fast ions are either born in a loss cone or evolve into it due to radial transport and/or pitch angle scattering. As shown in Fig. 8, prompt loss increases with decreasing plasma current and outer gap width. The loss also increases with decreasing tangency radius of the NB injectors. It is worth noting that prompt ion loss is not a linear function of the outer gap width, Δ_{gap}, but varies approximately as $\exp(-\Delta_{gap}/L)$ where L ~ 4 cm. As illustrated in Fig. 9, the scintillator Fast Loss Ion Probe (sFLIP) exhibits energetic ion loss during early beam injection at low plasma current, I_p ~ 500 kA. The gyroradius range, ρ ~ 25 cm, is consistent with ion loss at E_b = 90 keV in the ambient magnetic field of B = 0.25 T at the detector location. The pitch angle range, θ ~ 30°, indicates loss of trapped ions. This loss signal vanishes around t = 0.15 s as the plasma current is ramps above I_p ~ 700 kA.

Some other diagnostics on NSTX provide supporting evidence of energetic ion loss during early NB injection. The neutron production in NSTX is predominantly from beam-

target reactions. Thus the neutron rate is a robust measure of the energetic ion population. During early NB injection, the neutron yield is suppressed beyond what can be attributed to low values of the plasma density and temperature. The Charge Exchange Recombination Spectroscopy (CHERS) diagnostic shows that the toroidal rotation is also suppressed in this time interval. Thus both diagnostic measurements are consistent, albeit somewhat indirectly, with significant loss of energetic ions during early NB injection

3. TRANSP Analysis of NB Turn-on Energetic Ion Loss

In addition to a host of plasma parameters, the TRANSP code [15] is capable of simulating the NPA neutral flux measurements including horizontal and vertical scanning of the sightline. In this section, diagnostic measurements and TRANSP calculations will be compared to investigate the nature of early NB turn-on loss.

Fig. 10 shows the evolution of various quantities from diagnostic measurements and TRANSP calculations that are of relevance to understanding ion loss attending early NB injection, with the time of interest (TOI) denoted by the shaded vertical bar. From the top left panel, TRANSP simulation of the NPA signal (red) is in reasonable agreement with the NPA measurement (black). From the time of discharge initiation to the TOI, the measured outer gap width decreases by Δ_{Gap} = 13 cm and the calculated plasma volume increases by Δ_{Vol} = 3 m^3. During the TOI, the calculated orbit loss peaks (red) and the mean energy decreases for both the perpendicular (green) and parallel (blue) ion components. Early injection occurs at low values of $I_p \sim 0.5$ MA and $n_e \sim 1x10^{13} cm^{-3}$ in L-mode. Measured (black and tan) and calculated (red) neutron yields are low as is the

stored fast ion energy. Also during the TOI, the calculate NB torque drive (red) and measured toroidal rotation velocity (black) are suppressed due to elevated orbit torque loss (green). Note that the NPA measures the residual ion population and not the prompt loss ions, hence the anti-correlation between these quantities.

TRANSP calculation of power accounting for early NB injection corresponding to Fig. 10 is shown in Fig.11. In the TOI, early shine through (~ 20%) and orbit (~ 40%) losses reduce the effective NB heating to ~ 40% of P_{inj}. Although not shown, NB power lost to charge exchange is negligible at ~ 70 kW. According to TRANSP calculations, for early NB injection the deposition is core-weighted.

Fig. 12 illustrates the effect of outer gap excursion on ion loss attending early NB injection. As in Fig. 10, the evolution of various quantities from diagnostic measurements and TRANSP calculations are shown with the time of interest (TOI) denoted by the shaded vertical bar. From the top left panel, TRANSP simulation of the NPA signal (red) is in reasonable agreement with the NPA measurement (black). From the time of discharge initiation to the TOI, the variation of the measured out gap width, Δ_{Gap} = 7 cm and the calculated plasma volume, Δ_{Vol} = 1.2 m^3, are about half of that for Fig. 10. During the TOI, the calculated orbit loss (red) and the drop in the mean value of the perpendicular (green) and parallel (blue) ion energy components are reduced compared with Fig. 10. As before, injection occurs at low values of I_p ~ 0.5 MA and n_e ~ $1x10^{13}cm^{-3}$ in L-mode. During the TOI, measured (black) and calculated (red) neutron yields are low as is the stored fast ion energy. Also, NB power accounting shows reduced orbit loss. Thus avoiding outer gap excursions to small widths appears to reduce energetic ion loss during early NB injection.

The ion loss observed by the NPA varies with the sightline tangency radius. For the two discharges SN111478 and SN111482 shown in Fig. 13, the start-up parameters such as plasma current, electron density and outer gap excursion and so forth were very similar. For reference, the injected power (top panel) and calculated orbit loss (bottom panel) are shown in blue. The amplitude and evolution of the measured (black) and calculated (red) NPA signals, all at E_d = 70 keV, are significantly different for sightline tangency radii of R_{tan} = 120 cm (top panel) and R_{tan} = 80 cm (bottom panel). This suggests the existence of a spatial or pitch angle dependence to the ion loss observed by the NPA. Further evidence of this is provided by a shot-by-shot horizontal scan of the NPA diagnostic to obtain the charge exchange flux as a function of energy and tangency radius during early injection of Source B as shown in Fig. 14. The scan was performed over a sequence of shot ranging from SN111478 to SN111492. NB turn-on loss in the region of $E > E_b/2$ appears to be localized in the spatial range of $60 < R_{tan}$ (cm) < 115 (encircled region). As will be discussed next, this region corresponds to the NPA viewing primarily trapped particles.

TRANSP simulation of the NPA diagnostic is used to calculate the emissivity or source of the NPA signal as a function of distance along the NPA sightline. In Fig 15, the sum of the beam and edge neutral densities as a function of distance along the NPA sightline is shown by the green curves. The NB contribution is small as noted by its "location" along the NPA sightline. The fast ion distribution at E = 60 keV is shown by the ragged black curves. The product of the neutral and fast ion distributions yields the charge exchange emissivity shown by the red curve that is clearly edge-weighted. The correlation between distance along the NPA sightline and normalized minor radius is given

by the smooth black curve labeled r/a and the associated pitch is given by the blue curve. The bottom line is that NPA measurements of early beam loss are edge-weighted and correspond to trapped or barely trapped ion orbits.

4. Source Options for Early NB Turn-on

TRANSP modeling suggests different NB sources have different turn-on loss characteristics. EFIT [16 ,17] equilibria for SN112157 along with the tangency footprint of Source B are shown at the start of early NB injection (t = 80 ms) and 60 ms later are shown in Fig 16, illustrating the dynamic evolution of the plasma cross section, outer gap width and plasma volume during the start-up phase. This illustration suggests that using Source A for start-up, whose tangency radius is displaced ~ 10 cm closer to the plasma core, might have an advantage in reducing the shine-through and orbit loss relative to Source B. To investigate this conjecture, the energetic ion loss was examined for several dischages that were nominally identical except that different, single, NB sources were used for early injection.

In Fig. 17, the use of Source A (SN112164) versus Source B (SN112159) for early beam injection is compared. (Though not shown in detail, Source C proved to be clearly inferior.) The discharge parameters from the top left, I_p, n_e, P_b, and Δ_{Gap} are identical for both discharges. The NPA signal at E_D = 80 keV showed relatively reduced ion loss for Source A compared with either Source B or Source C. TRANSP power accountability shows that at 20 ms after turn-on, Source A delivered 300 kW more heating power than Source B, a 50 % gain due to a reduction in shine through and orbit losses. In the

absence of possible other deleterious effects, it would appear that Source A would give better performance as the early start-up beam.

5. Summary

Early neutral beam injection is used in NSTX to heat the electrons and slow current penetration which keeps q(0) elevated to avoid deleterious MHD activity and at the same time reduces Ohmic flux consumption, all of which aids long pulse operation. However, the low plasma current ($I_p \sim 0.5$ MA) and electron density ($n_e \sim 1x10^{13}cm^{-3}$) attending early injection lead to elevated orbit and shine through losses. For NB injection, whether early or late, n=1, 2 MHD activity at f ~ 50 kHz typically sets in at ~ 20 ms after start of injection. This activity appears to be benign since no evidence has emerged so far to indicate the existence of any anomalous energetic ion loss processes. The inherent orbit losses are aggravated by large excursions to small outer gap widths during current ramp up. Better gap control is possible as demonstrated in experiments using HHFW heating. TRANSP analysis indicated that orbit loss could be reduced by ~ 50% by using Source A for start-up rather than Source B. Since Source A is the designated beam for MSE measurements, it could well be the preferred source provided there are not other offsetting deleterious elements such as MHD activity.

Acknowledgement

This work was supported by the United States Department of Energy under contract number DE-AC02-76CH03073.

References

[1] Peng Y.-K. M. and Strickler D. J., 1986 Nucl. Fusion **26** 769.

[2] Ono M., *et al.,* 2001 Nucl. Fusion **41** 1435

[3] Gates D. A., *et al.*, "Progress Towards Steady State on NSTX," Princeton Plasma Physics Report PPPL-4044 (2005). Submitted to Nucl. Fusion.

[4] Menard J. E., *et al.,* "Internal Kink Mode Dynamics in High-beta NSTX Plasmas," Princeton Plasma Physics Report PPPL-4035 (2004). Submitted to Nucl. Fusion.

[5] Darrow D. S., *et al.*, "Neutral Beam Ion Loss Modeling for NSTX," Controlled Fusion and Plasma Physics (Proc. of the 26th EPS Conf., Maastricht, 1999), ECA Vol. **23J**, European Physical Society, Geneva, (1999). CD-ROM file P4.090

[6] Darrow D. S., Bell R., Johnson D. W., Kugel H., Wilson J. R., Cecil F. E., Maingi R., Krasilnikov A., and Alekseyev A., 2001 Rev. Sci. Instrum. 72, 784

[7] Darrow D. S., *et al.*, "Measurements of Prompt and MHD-Induce Fast Ion Loss from National Spherical Torus Experiment Plasmas," Fusion Energy 2002 (Proc. 19th Int. Conf. Lyon, 2002) (Vienna: IAEA) CD-ROM fileEX/P2-01and http://www.iaea.org/programmes/ripc/physics/fec2002/html/fec2002.htmI

[8] Medley S. S., *et al.,* 2004 Rev. Sci. Instrum. **75** 3625

[9] Medley S. S. and Roquemore A. L., 1998 Rev. Sci. Instrum. **69** 2651

[10] Medley S. S., *et al.,* 2003 Rev. Sci. Instrum. **74** 1896

[11] Medley S. S. , *et al.,* 2004 Nucl. Fusion **44** 1158

[12] Shinohara K., *et al.,* 2004 Rev. Sci. Instrum. **75** 3640

[13] Darrow D. S., 2004 Bull. Amer. Phys. Soc. **41**(8) 301

[14] Spitzer L. Jr., Physics of Fully Ionized Gases, Interscience, New York (1962)

[15] Onega J., Evrard M., McCune D., 1998 Transactions of Fusion Technology **33** 182

[16] Lao L. L., *et al.,* 1985 Nucl. Fusion **25** 1611

[17] Sabbagh S. A., *et al.,* 2001 Nucl. Fusion **41** 1601

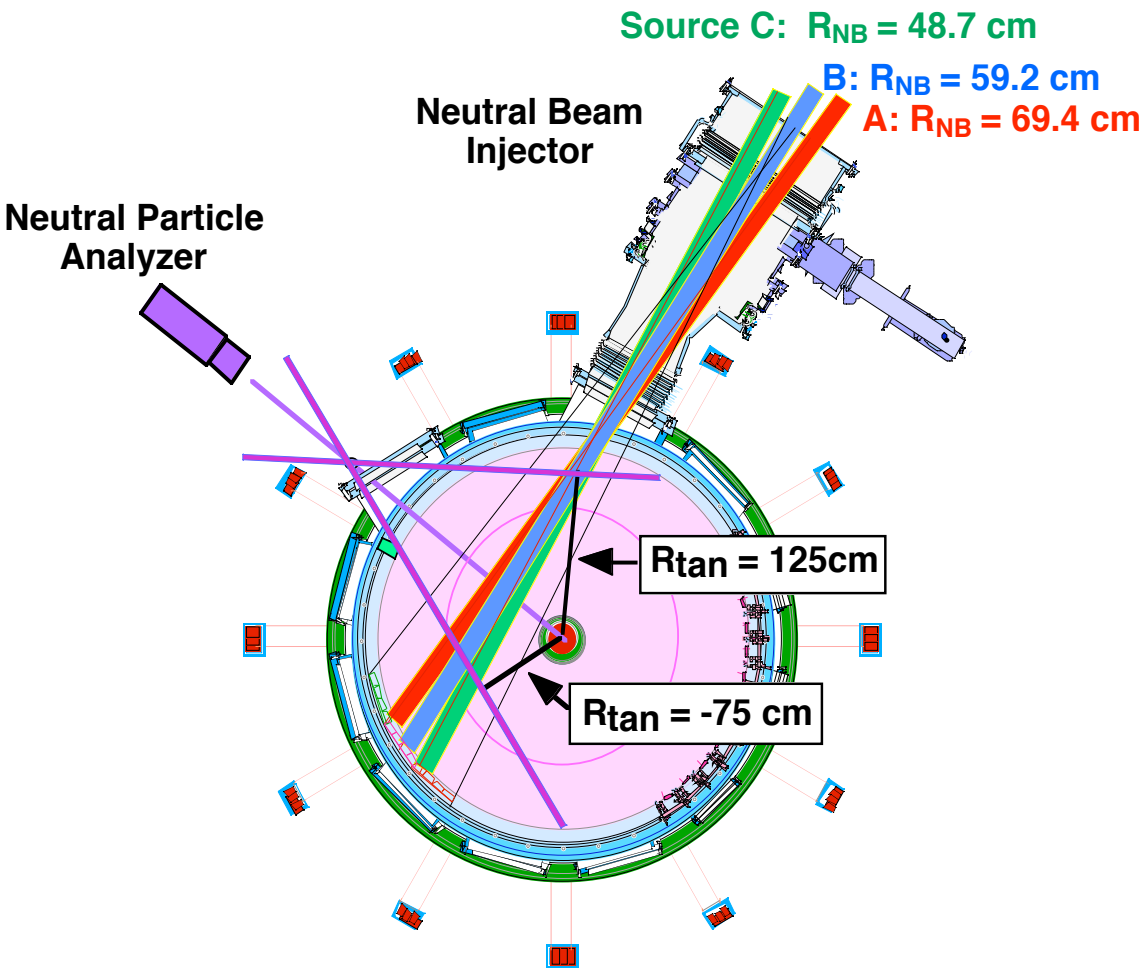

Figure 1. The Neutral Particle Analyzer (NPA) on NSTX views across the three neutral beam injection sources and can be scanned over a wide range of sightline tangency radii, R_{tan}, on a shot-to-shot basis. R_{tan}, is the perpendicular distance between the machine center and the NPA sightline. Positive (negative) values of R_{tan}, view co(counter)-going ions.

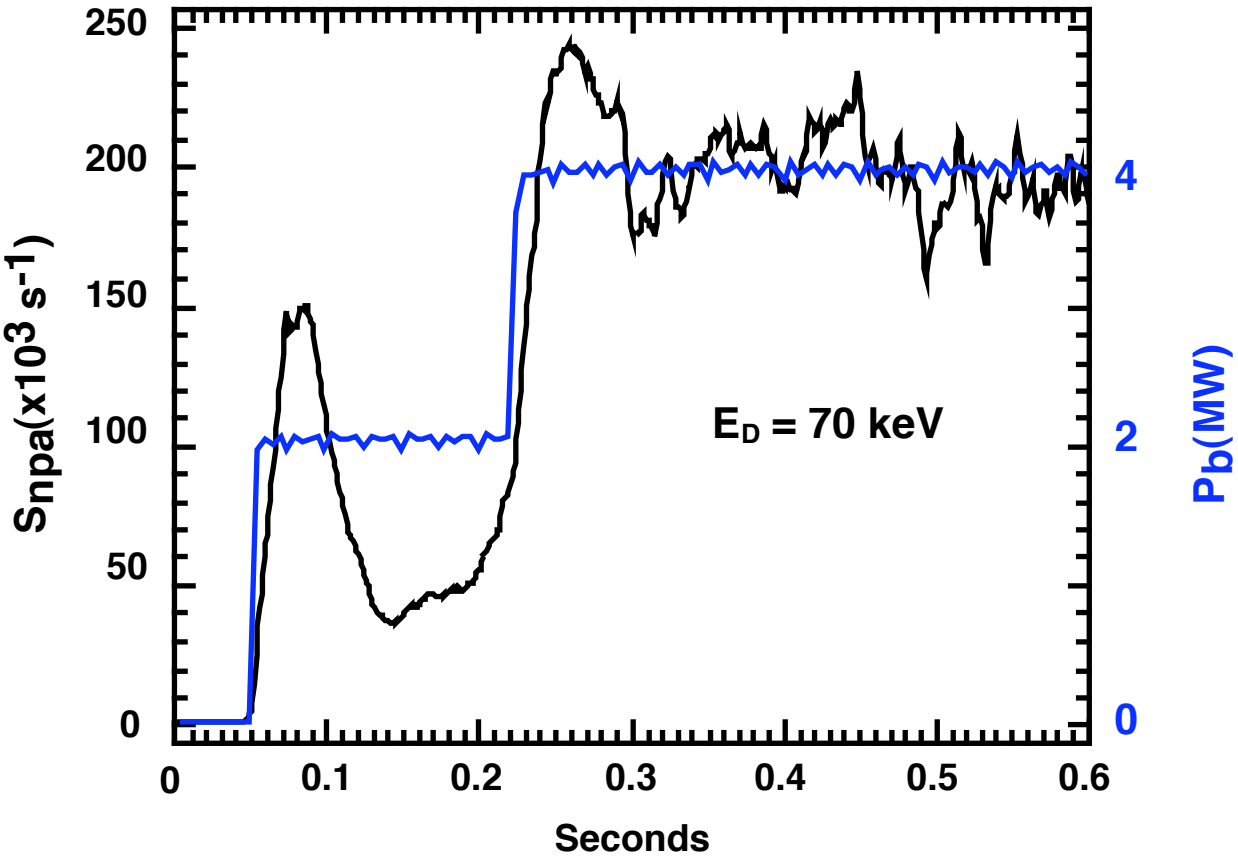

Figure 2. Shown is the NPA flux signal at E_D = 70 keV and the waveform for neutral beam injection. Source B with E_b = 88 keV is turned on at t = 50 ms followed by Source A with E_b = 88 keV at 200 ms. Initially the NPA signal shows a "normal" rise but then suddenly drops by ~ 70% followed by a recovery phase up to turn-on of the second beam. This is not a detector saturation effect, since even higher signal levels are sustained after turn-on of the second NB. The second beam may also exhibit turn-on loss, but very modest compared with the first beam.

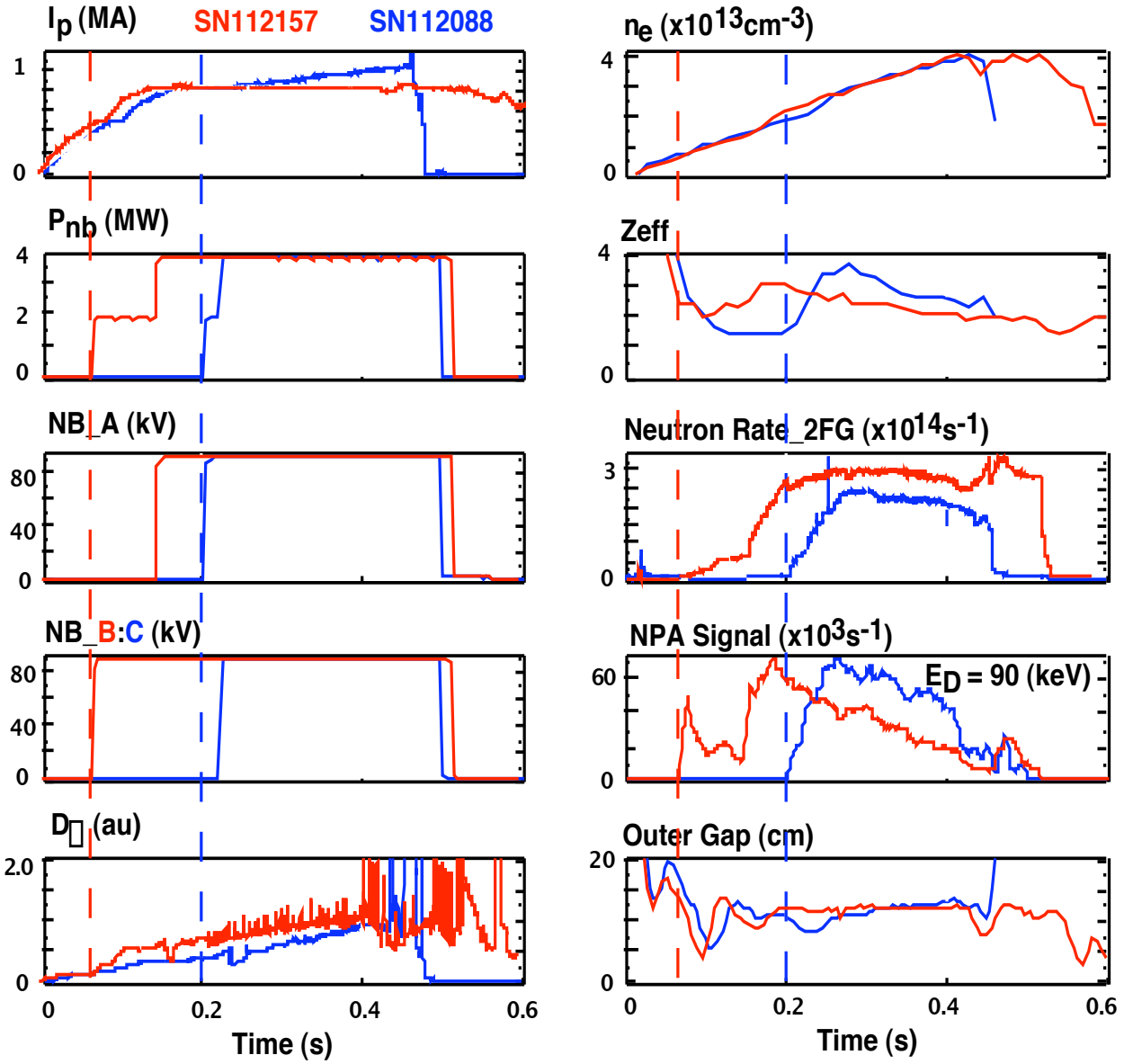

Figure 3. Discharges with early (SN112157 in red) and late (SN112088 in blue) NB injection are compared. In the time of interest up to t ~ 300 ms, both discharges are similar with regard to plasma current, electron density, beam energy and injected power and outer gap evolution. For late injection, the NPA signal and the neutron rate rise smoothly to a plateau. For early injection, however, the initial rise in the NPA signal quickly collapses and neutron production is minimal.

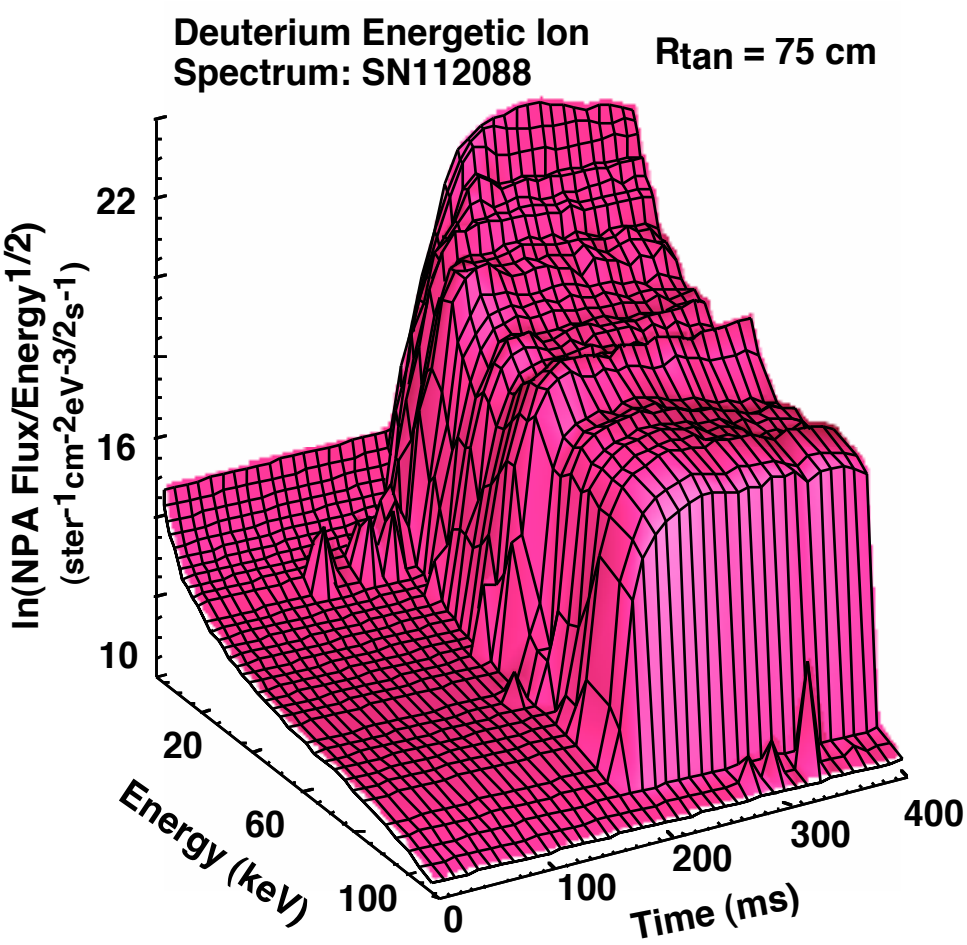

Figure 4. Shown is the 3D spectrum of the NPA flux versus deuterium ion energy and time for the late injection case. The point to note is that following beam turn-on the flux rises smoothly at all energies and rolls over to an equilibrium distribution.

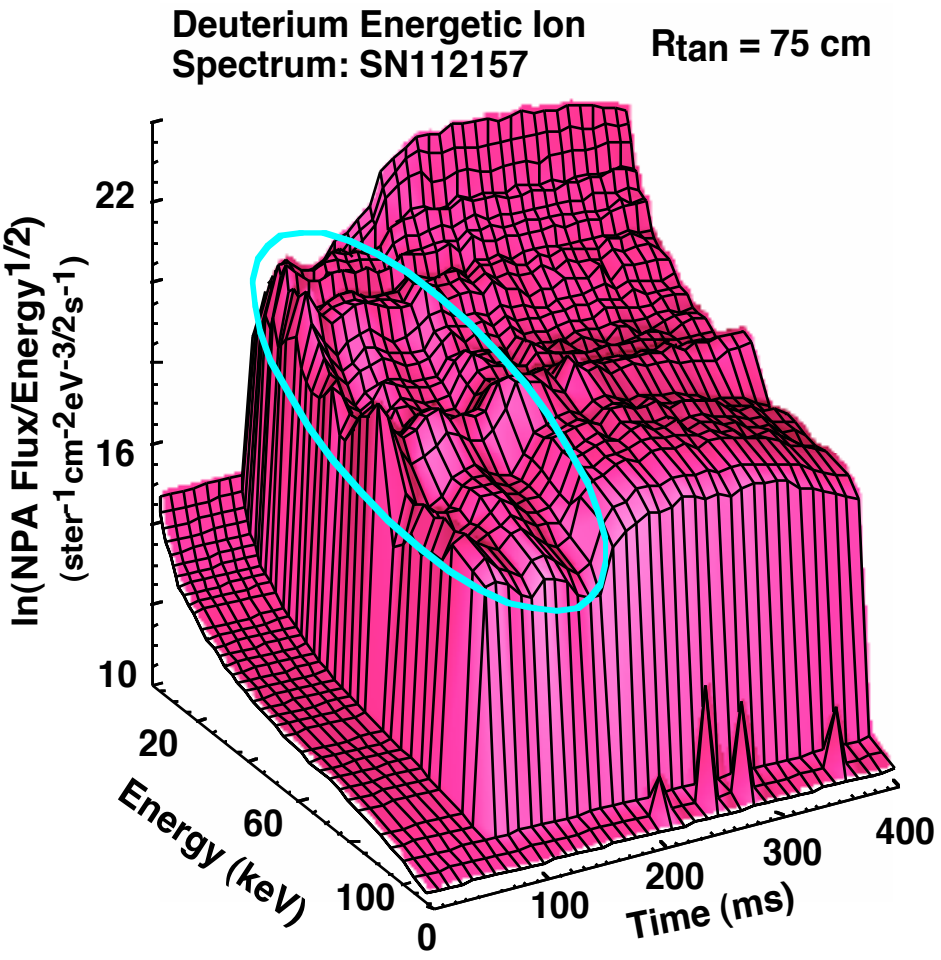

Figure 5. Shown is the 3D spectrum of the NPA flux versus deuterium ion energy and time for the early injection case. The point to note is that following beam turn-on the flux rises promptly at all energies but then collapses and "wobbles" (encircled region). When the second beam is turned on at t = 200 ms, the flux rises smoothly and rolls over to an equilibrium distribution as seen in the late turn-on case in Fig. 4.

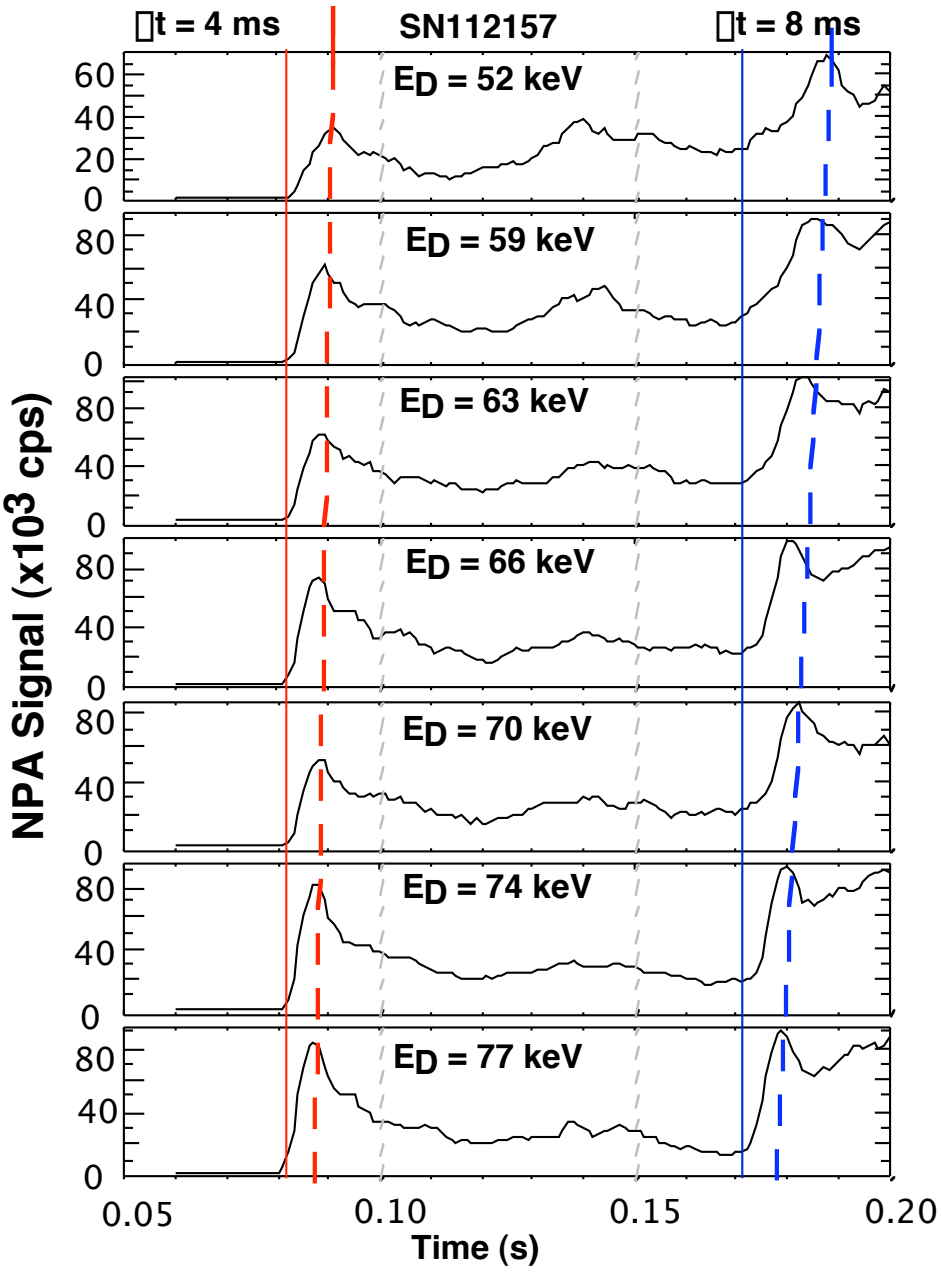

Figure 6. The NPA signal is shown for a selection of channels in the energy range $E_b/2 < E \leq E_b$) for SN112157. The solid red and blue lines mark the turn-on of the first and second beams, respectively. The dashed lines track the delay, Δt, in the signal peaking with decreasing energy. This is simply the effect of classical ion slowing down. This behavior provides supporting evidence the NPA signal is "real": e.g. not a detector saturation effect.

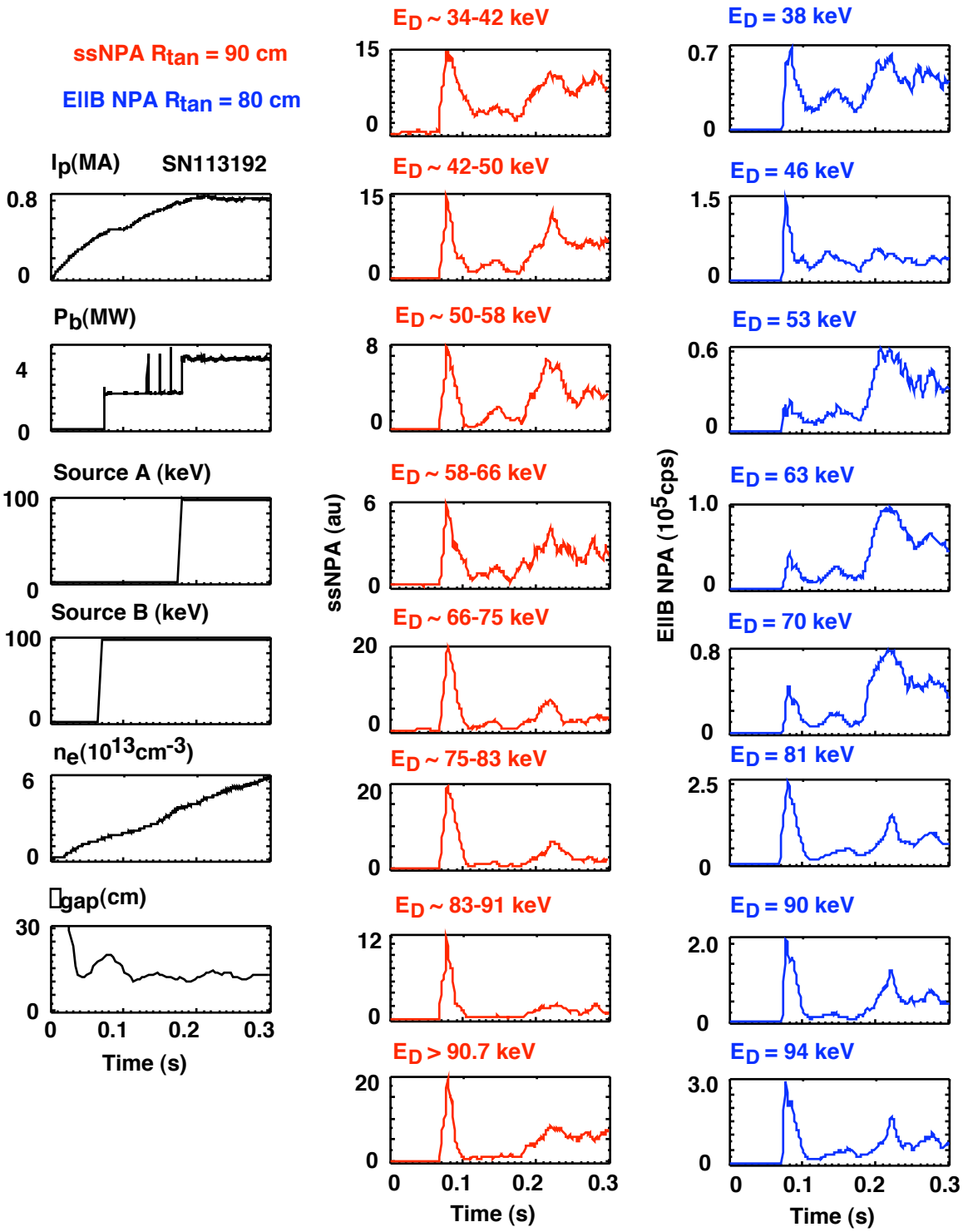

Figure 7 The Solid State Neutral Particle Analyzer (ssNPA) on NSTX exhibits the same time evolution following early beam injection as the EIIB NPA. Since different detectors are used in the two systems, this provides further evidence against detector saturation effects.

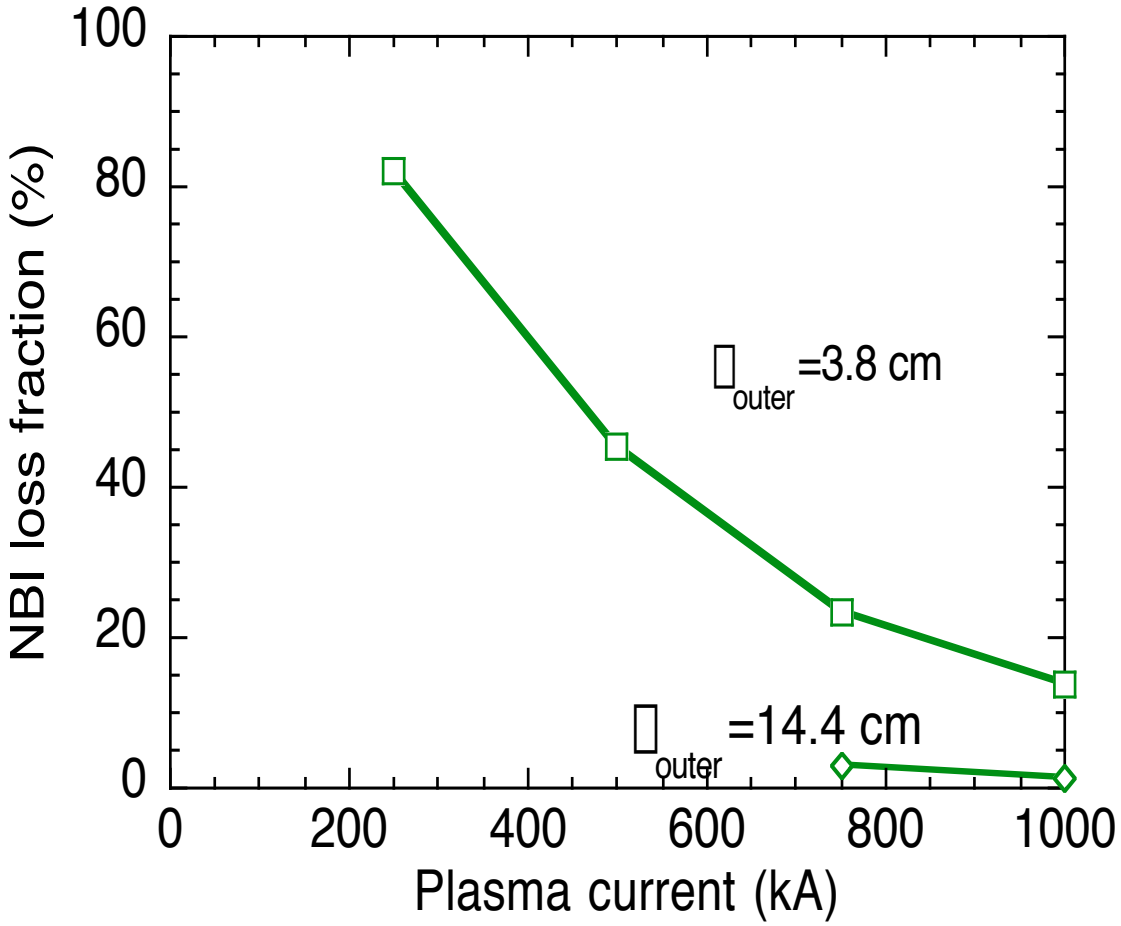

Figure 8. ORBIT code analysis shows that prompt orbit loss occurs when fast ions are either born in a loss cone or evolve into it due to radial transport and/or pitch angle scattering. As shown in the figure, prompt loss increases with degreasing plasma current and outer gap width. The loss also increases with decreasing tangency radius of the NB injectors.

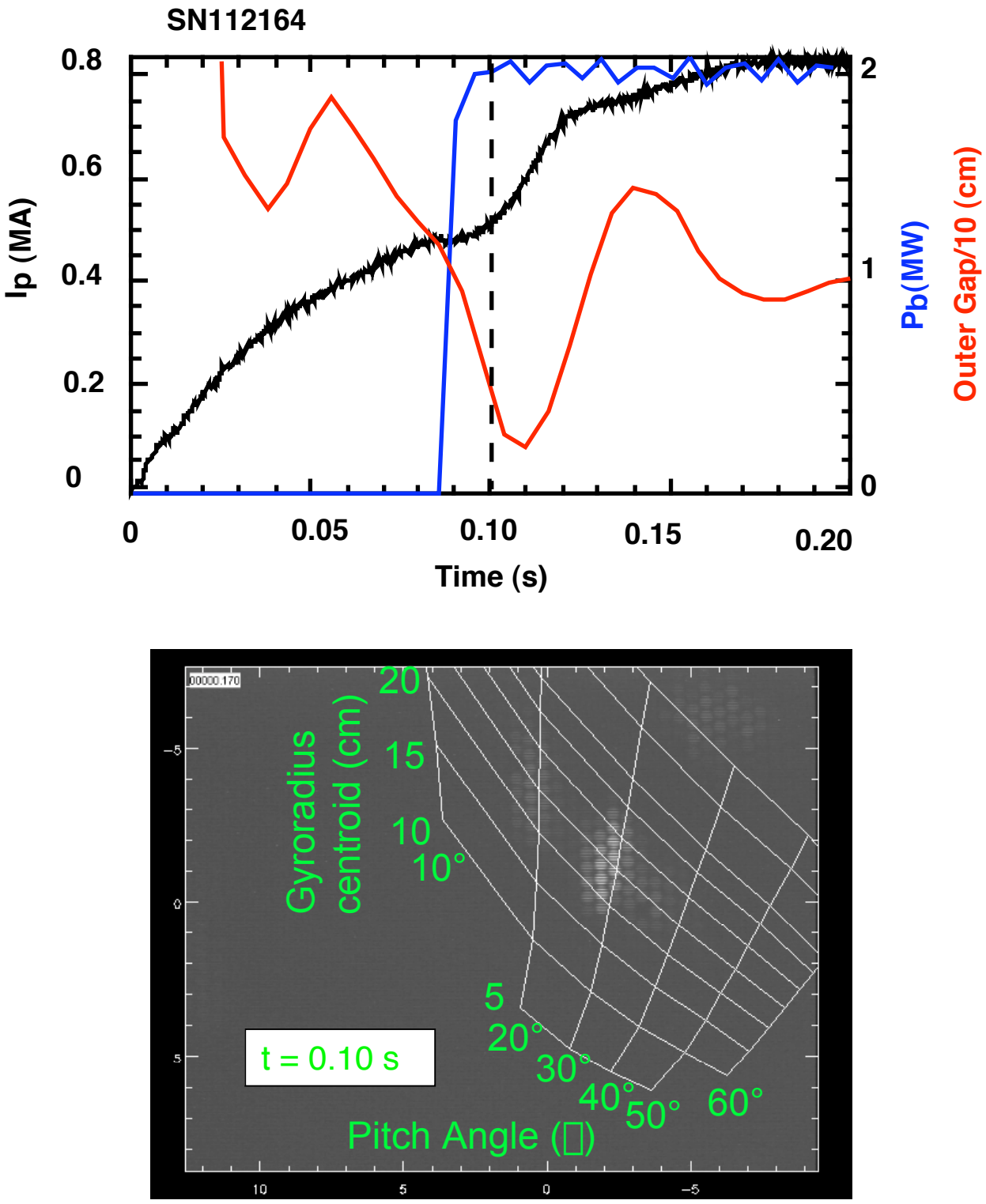

Figure 9. The scintillator Fast Loss Ion Probe (sFLIP) exhibits energetic ion loss during early beam injection at low plasma current, I_p ~ 500 kA. This loss signal vanishes around 0.15 s as the current is ramps above I_p ~700 kA.

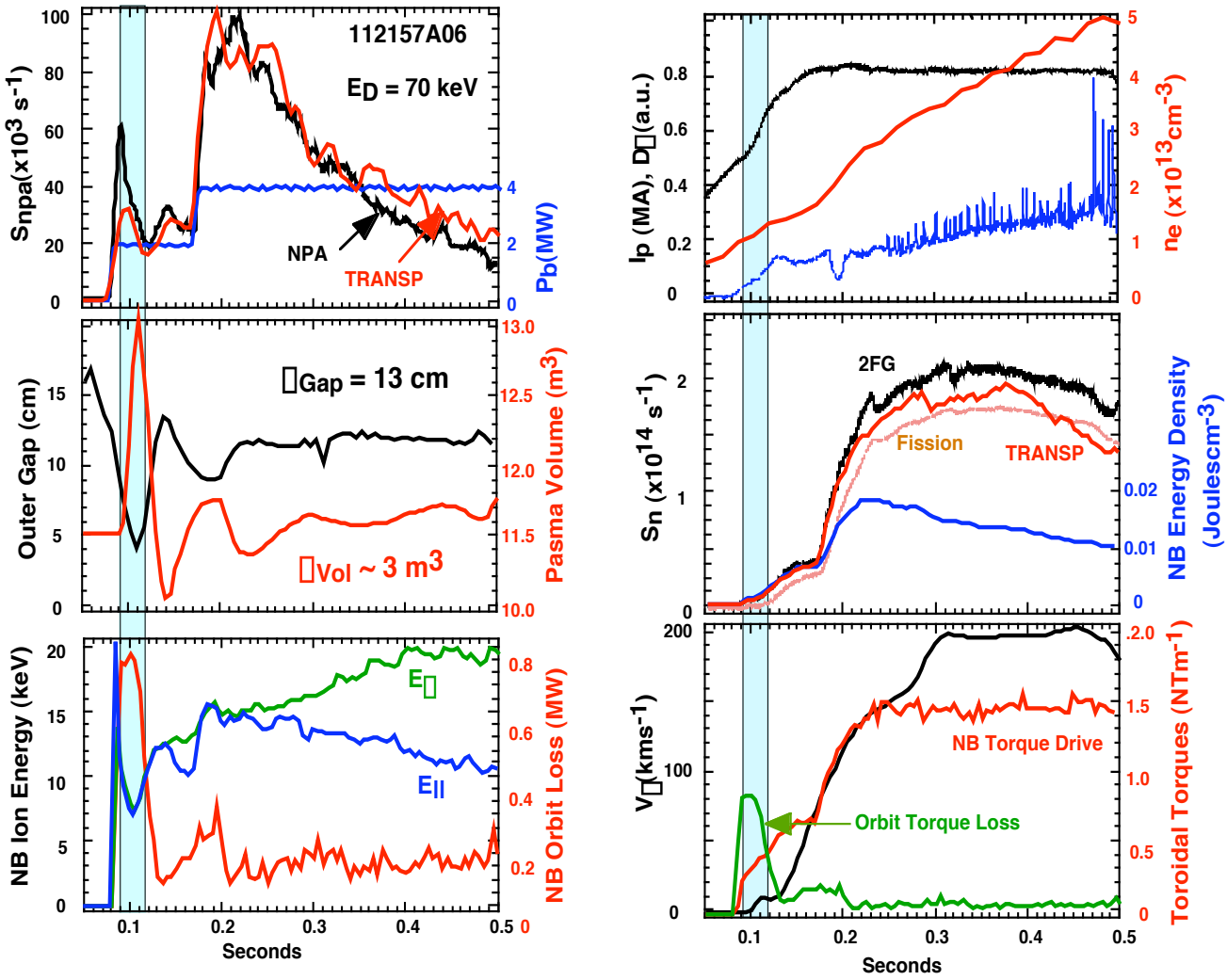

Figure 10. The evolution of various quantities from diagnostic measurements and TRANSP calculations of relevance to understanding ion loss attending early NB injection are shown with the time of interest (TOI) denoted by the shaded vertical bar. From the top left panel, TRANSP simulation of the NPA signal (red) is in reasonable agreement with the NPA measurement (black). From the time of discharge initiation to the TOI, the measured outer gap width decreases by Δ_{Gap} = 13 cm and the calculated plasma volume increases by Δ_{Vol} = 3 m^3. During the TOI, the calculated orbit loss peaks (red) and the mean energy decreases for both the perpendicular (green) and parallel (blue) ion components. Early injection occurs at low values of $I_p \sim 0.5$ MA and $n_e \sim 1 \times 10^{13}$cm^{-3} in L-mode. Measured (black and tan) and calculated (red) neutron yields are low as is the stored fast ion energy. Also during the TOI, the calculated NB torque drive (red) and measured toroidal rotation velocity (black) are suppressed due to elevated orbit torque loss (green). Note that the NPA measures the residual ion population and not the prompt loss ions, hence the anti-correlation between these quantities.

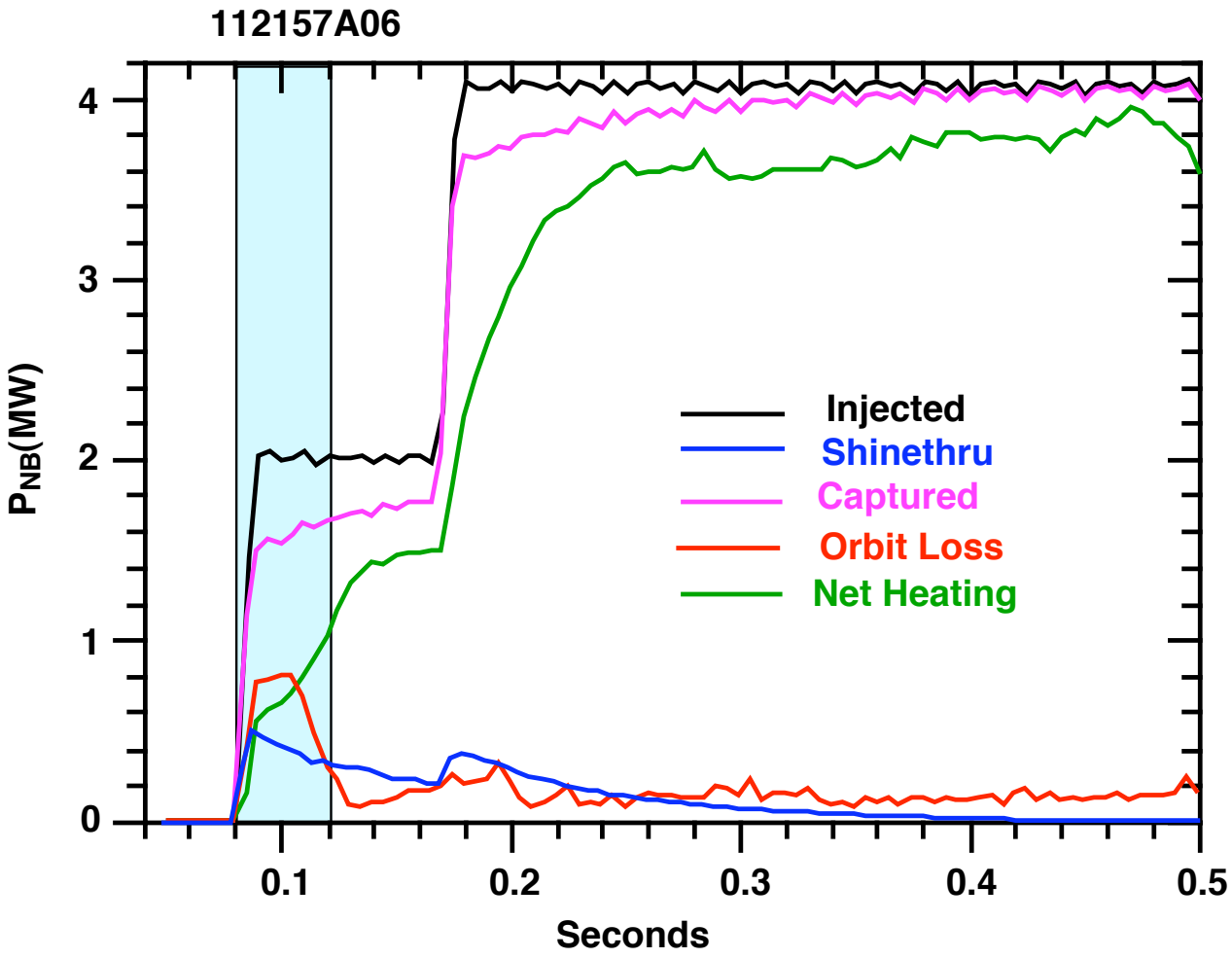

Figure 11. TRANSP calculation of power accounting for early NB injection corresponding to Fig. 10 is shown. In the TOI, early shine through (~ 20%) and orbit (~ 40%) losses reduce the effective NB heating to ~ 40% of P_{inj}. Although not shown, NB power lost to charge exchange is negligible at ~ 70 kW. According to TRANSP calculations, for early NB injection the deposition is core-weighted.

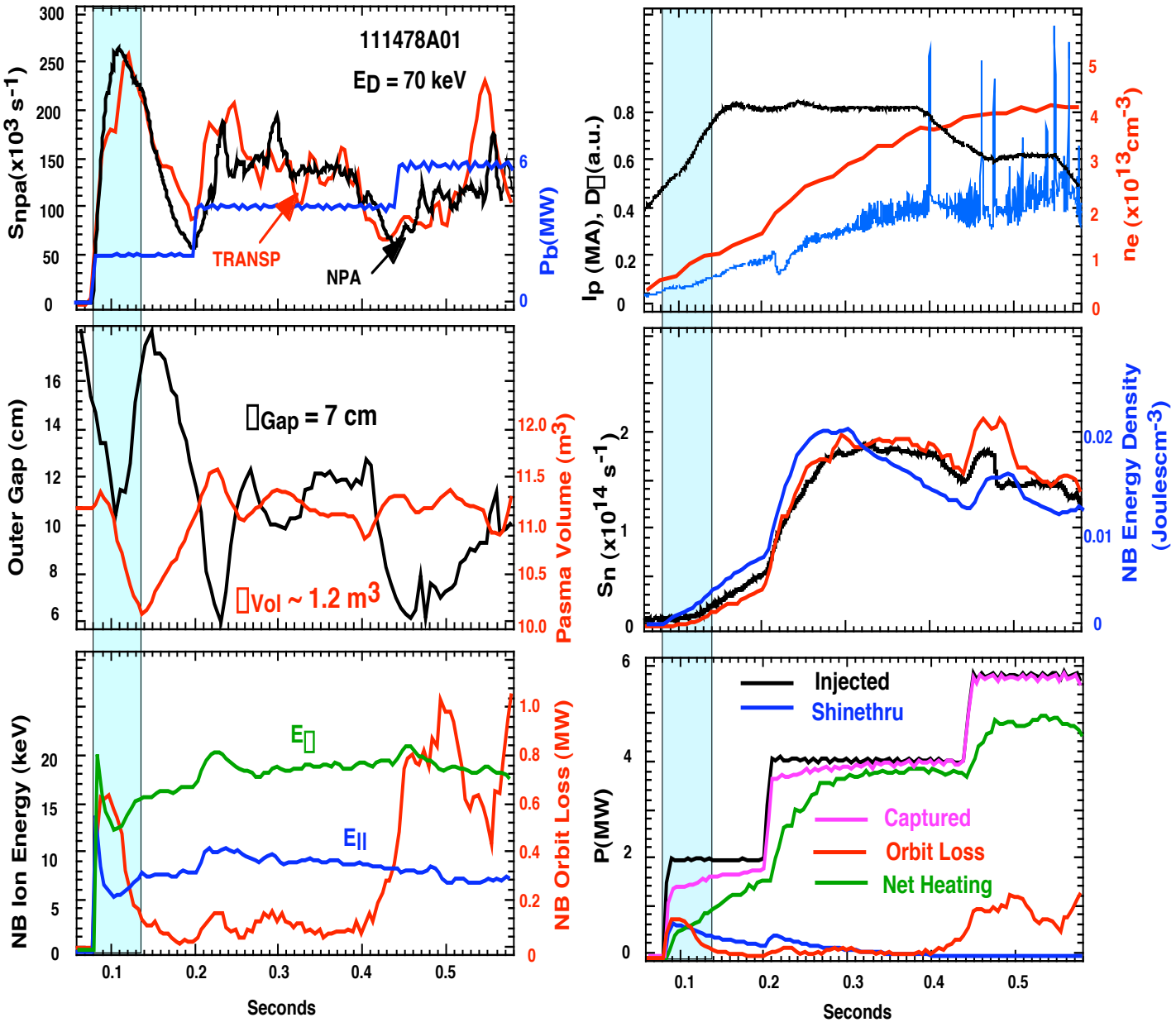

Figure 12. This figure illustrates the effect of outer gap excursion on ion loss attending early NB injection. As in Fig. 10, the evolution of various quantities from diagnostic measurements and TRANSP calculations are shown with the time of interest (TOI) denoted by the shaded vertical bar. From the top left panel, TRANSP simulation of the NPA signal (red) is in reasonable agreement with the NPA measurement (black). From the time of discharge initiation to the TOI, the variations of the measured out gap width, Δ_{Gap} = 7 cm and the calculated plasma volume, Δ_{Vol} = 1.2 m^3, are about half of that for Fig. 10. During the TOI, the calculated orbit loss (red) and the drop in the mean value of the perpendicular (green) and parallel (blue) ion energy components are reduced compared with Fig. 10. As before, injection occurs at low values of $I_p \sim 0.5$ MA and $n_e \sim 1\text{x}10^{13}\text{cm}^{-3}$ in L-mode. During the TOI, measured (black) and calculated (red) neutron yields are low as is the stored fast ion energy. Also, NB power accounting shows reduced orbit loss.

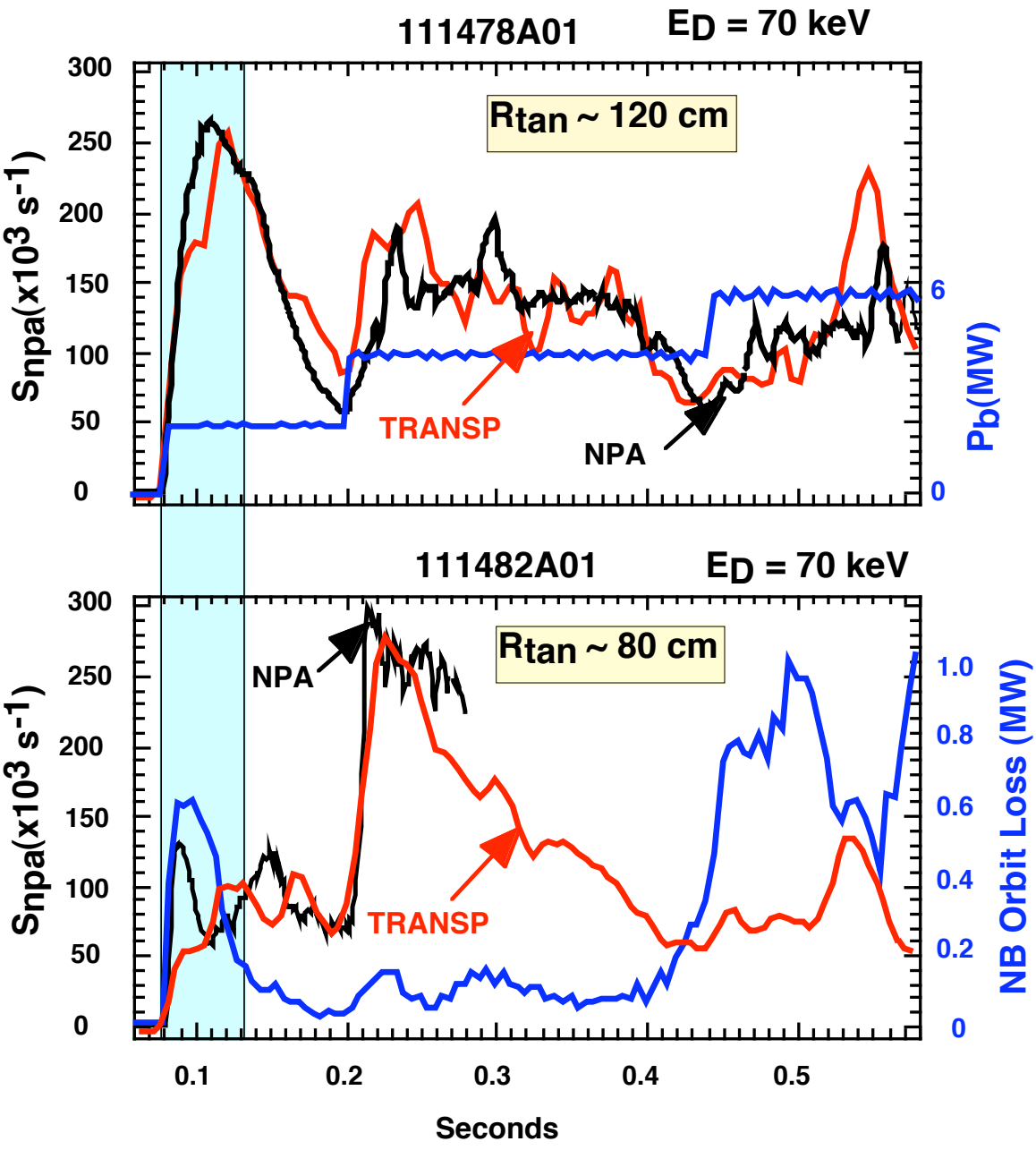

Figure 13. The ion loss observed by the NPA varies with the sightline tangency radius, suggesting the existence of a spatial or pitch angle dependence. For the two discharges shown, SN111478 and SN111482, the start-up parameters such as plasma current, electron density, outer gap excursion and so forth were very similar. For reference, the injected power (top panel) and calculated orbit loss (bottom panel) are shown in blue. The amplitude and evolution of the measured (black) and calculated (red) NPA signals, all at E_d = 70 keV, are significantly different for sightline tangency radii of R_{tan} = 120 cm (top panel) and R_{tan} = 80 cm (bottom panel).

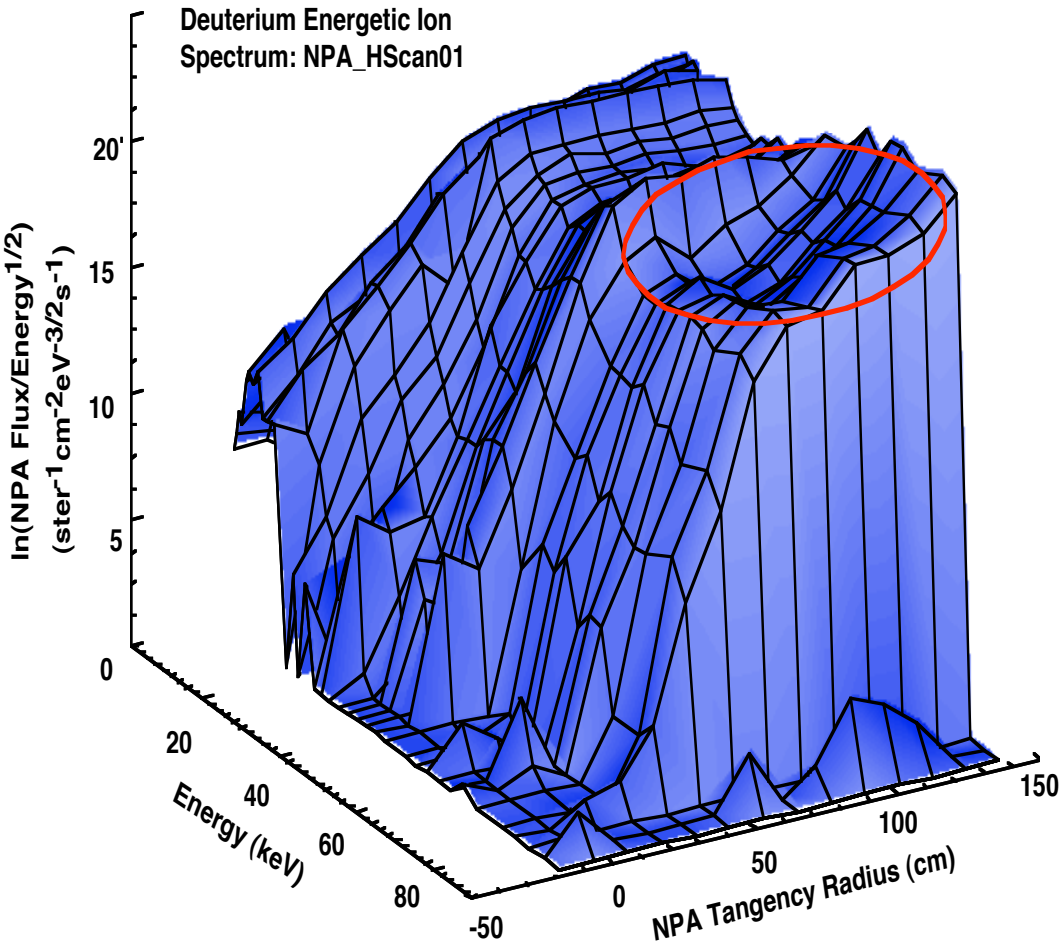

Figure 14. A shot-by-shot horizontal scan of the NPA diagnostic was performed to obtain the charge exchange flux as a function of energy and tangency radius during early injection of Source B in a discharge sequence ranging from SN111478 to SN111492. NB turn-on loss in the region of $E > E_b/2$ appears to be localized in the spatial range of $60 < R_{tan}$ (cm) < 115 (encircled region).

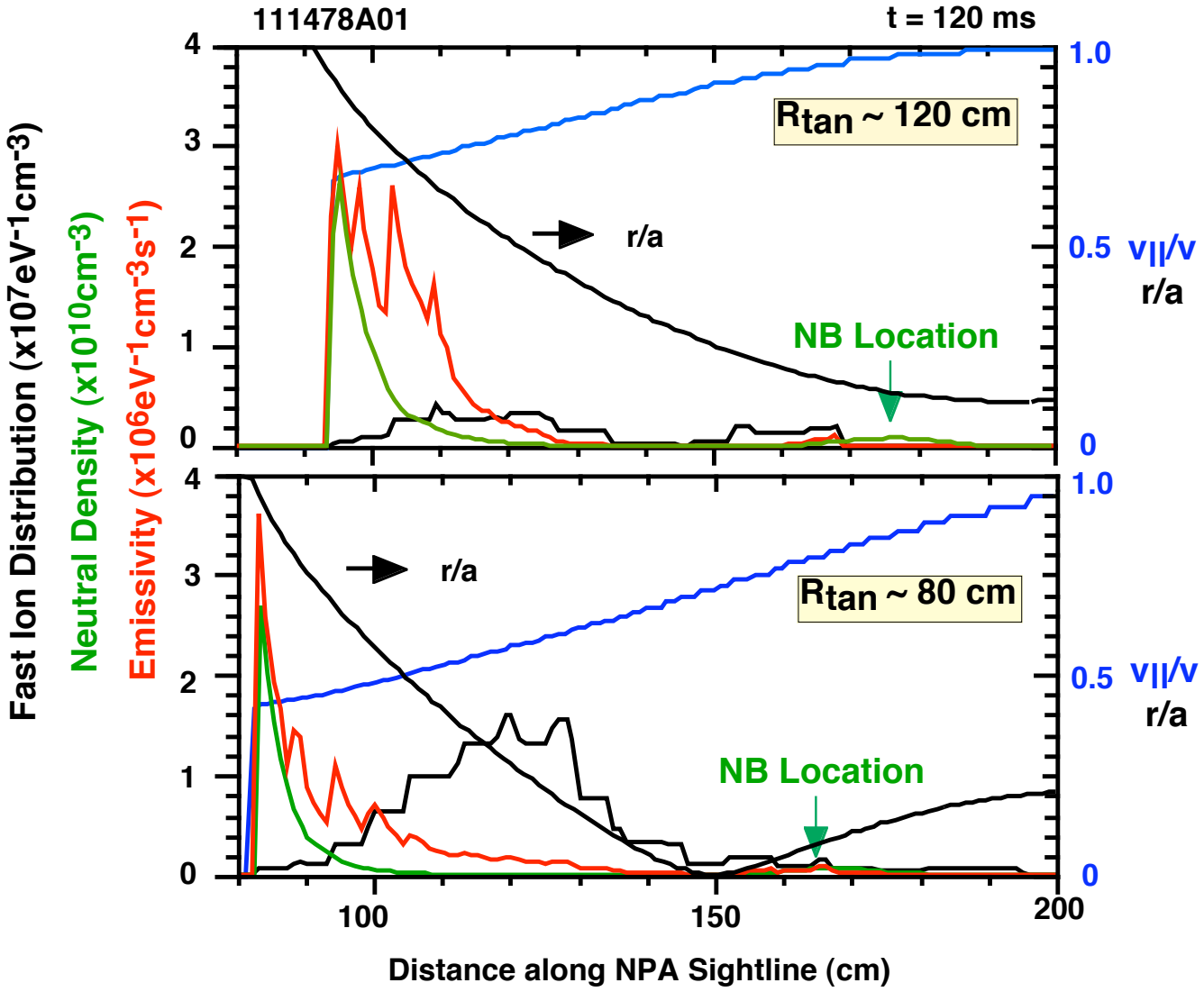

Figure 15. TRANSP simulation of the NPA diagnostic is used to calculate the emissivity or source of the NPA signal as a function of distance along the NPA sightline. The sum of the beam and edge neutral densities is shown by the green curves. The NB contribution is small as noted by its "location" along the NPA sightline. The fast ion distribution at E = 60 keV is shown by the ragged black curves. The product of the neutral and fast ion distributions yields the charge exchange emissivity shown by the red curve that is clearly edge-weighted. The correlation between distance along the NPA sightline and normalized minor radius is given by the smooth black curve labeled r/a and the associated pitch is given by the blue curve. The bottom line is that NPA measurements of early beam loss are edge-weighted and correspond to trapped or barely trapped ion orbits.

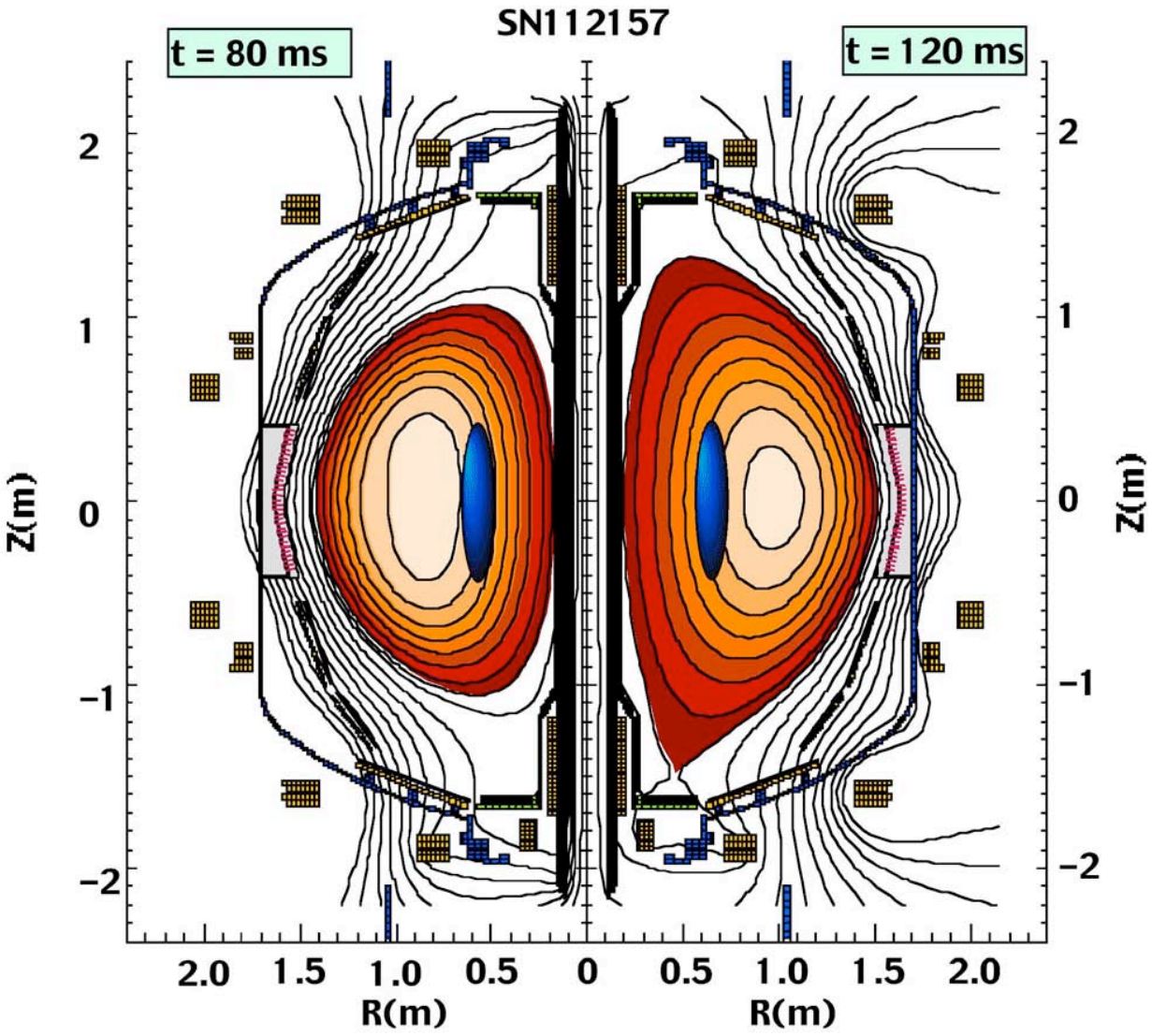

Figure 16. EFIT equilibria for SN112157 along with the tangency footprint of Source B are shown at the start of early NB injection (t = 80 ms) and 60 ms later, illustrating the dynamic evolution of the plasma cross section, outer gap width and plasma volume during the start-up phase. This illustration suggests that using Source A for start-up, whose tangency radius is displaced ~ 10 cm closer to the plasma core, might have an advantage in reducing the shine-through and orbit loss relative to Source B.

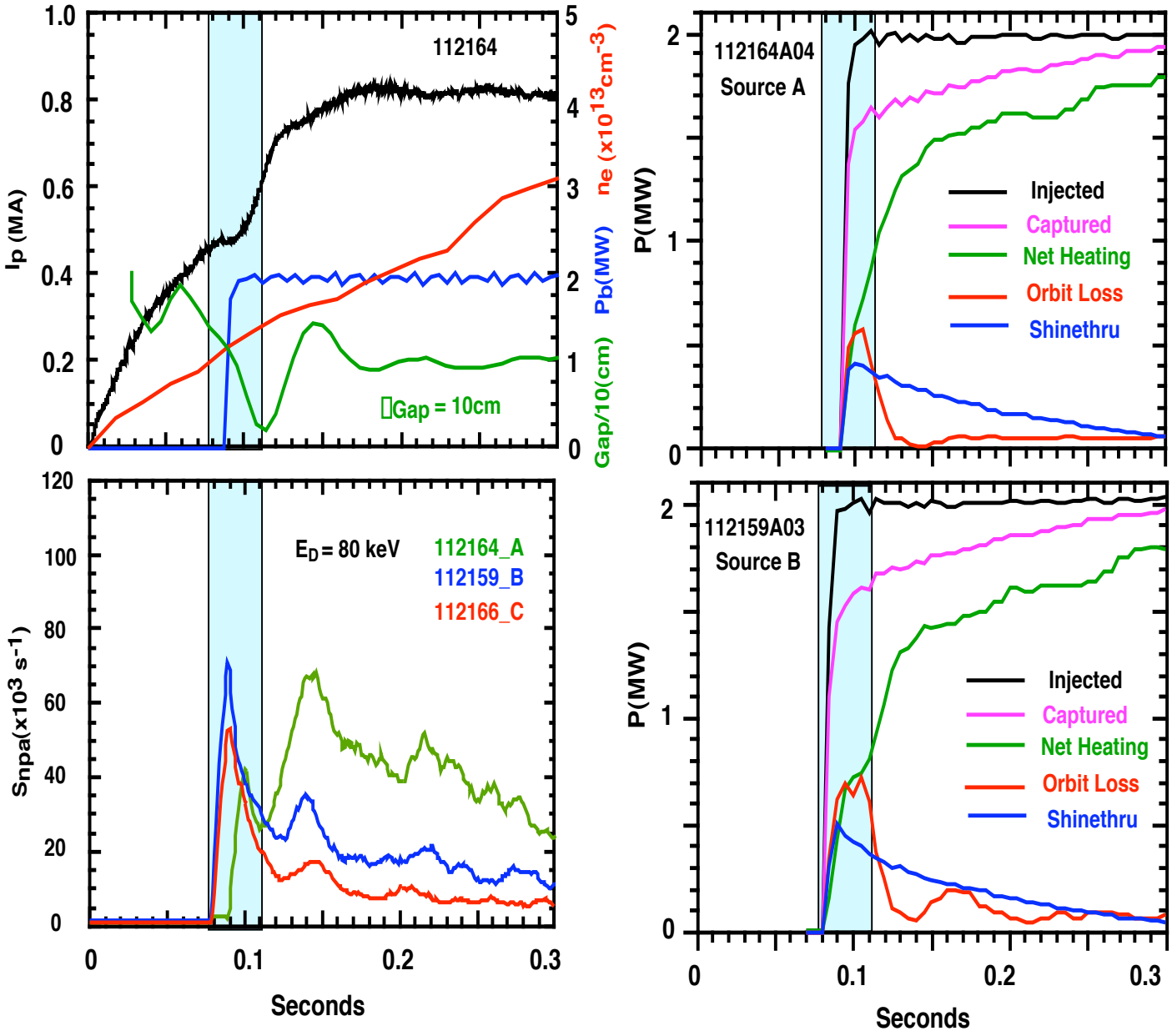

Figure 17. Use of Source A (SN112164) versus Source B (SN112159) for early beam injection is compared (Source C is clearly inferior). The discharge parameters from the top left, I_p, n_e, P_b, and Δ_{Gap} are identical for both discharges. The NPA signal at E_D = 80 keV showed relatively reduced ion loss for Source A compared with either Source B or Source C. TRANSP power accountability shows that at 20 ms after turn-on, Source A delivered 300 kW more heating power than Source B, a 50 % gain due to a reduction in shine through and orbit losses.

External Distribution

Plasma Research Laboratory, Australian National University, Australia

Professor I.R. Jones, Flinders University, Australia

Professor João Canalle, Instituto de Fisica DEQ/IF - UERJ, Brazil

Mr. Gerson O. Ludwig, Instituto Nacional de Pesquisas, Brazil

Dr. P.H. Sakanaka, Instituto Fisica, Brazil

The Librarian, Culham Science Center, England

Mrs. S.A. Hutchinson, JET Library, England

Professor M.N. Bussac, Ecole Polytechnique, France

Librarian, Max-Planck-Institut für Plasmaphysik, Germany

Jolan Moldvai, Reports Library, Hungarian Academy of Sciences, Central Research Institute for Physics, Hungary

Dr. P. Kaw, Institute for Plasma Research, India

Ms. P.J. Pathak, Librarian, Institute for Plasma Research, India

Dr. Pandji Triadyaksa, Fakultas MIPA Universitas Diponegoro, Indonesia

Professor Sami Cuperman, Plasma Physics Group, Tel Aviv University, Israel

Ms. Clelia De Palo, Associazione EURATOM-ENEA, Italy

Dr. G. Grosso, Instituto di Fisica del Plasma, Italy

Librarian, Naka Fusion Research Establishment, JAERI, Japan

Library, Laboratory for Complex Energy Processes, Institute for Advanced Study, Kyoto University, Japan

Research Information Center, National Institute for Fusion Science, Japan

Dr. O. Mitarai, Kyushu Tokai University, Japan

Dr. Jiangang Li, Institute of Plasma Physics, Chinese Academy of Sciences, People's Republic of China

Professor Yuping Huo, School of Physical Science and Technology, People's Republic of China

Library, Academia Sinica, Institute of Plasma Physics, People's Republic of China

Librarian, Institute of Physics, Chinese Academy of Sciences, People's Republic of China

Dr. S. Mirnov, TRINITI, Troitsk, Russian Federation, Russia

Dr. V.S. Strelkov, Kurchatov Institute, Russian Federation, Russia

Professor Peter Lukac, Katedra Fyziky Plazmy MFF UK, Mlynska dolina F-2, Komenskeho Univerzita, SK-842 15 Bratislava, Slovakia

Dr. G.S. Lee, Korea Basic Science Institute, South Korea

Dr. Rasulkhozha S. Sharafiddinov, Theoretical Physics Division, Insitute of Nuclear Physics, Uzbekistan

Institute for Plasma Research, University of Maryland, USA

Librarian, Fusion Energy Division, Oak Ridge National Laboratory, USA

Librarian, Institute of Fusion Studies, University of Texas, USA

Librarian, Magnetic Fusion Program, Lawrence Livermore National Laboratory, USA

Library, General Atomics, USA

Plasma Physics Group, Fusion Energy Research Program, University of California at San Diego, USA

Plasma Physics Library, Columbia University, USA

Alkesh Punjabi, Center for Fusion Research and Training, Hampton University, USA

Dr. W.M. Stacey, Fusion Research Center, Georgia Institute of Technology, USA

Dr. John Willis, U.S. Department of Energy, Office of Fusion Energy Sciences, USA

Mr. Paul H. Wright, Indianapolis, Indiana, USA

The Princeton Plasma Physics Laboratory is operated
by Princeton University under contract
with the U.S. Department of Energy.

Information Services
Princeton Plasma Physics Laboratory
P.O. Box 451
Princeton, NJ 08543

Phone: 609-243-2750
Fax: 609-243-2751
e-mail: pppl_info@pppl.gov
Internet Address: http://www.pppl.gov